Water Research 202 (2021) 117429

Contents lists available at ScienceDirect

Water Research

journal homepage: www.elsevier.com/locate/watres

Characterizing the multidimensionality of microplastics across environmental compartments

Merel Kooi [a,*], Sebastian Primpke [b], Svenja M. Mintenig [a], Claudia Lorenz [c], Gunnar Gerdts [b], Albert A. Koelmans [a]

[a] Aquatic Ecology and Water Quality Management Group, Wageningen University & Research, The Netherlands
[b] Shelf Seas Systems Ecology, Alfred Wegener Institute Helmholtz Centre for Polar and Marine Research, Germany
[c] Department of The Built Environment, Aalborg University, Thomas Manns Vej 23, 9220 Aalborg Øst, Denmark

ARTICLE INFO

Keywords:
Microplastics
Probability density functions
Size distribution
Risk assessment
Environment
Human health

ABSTRACT

Understanding the multidimensionality of microplastics is essential for a realistic assessment of the risks these particles pose to the environment and human health. Here, we capture size, shape, area, polymer, volume and mass characteristics of >60,000 individual microplastic particles as continuous distributions. Particles originate from samples taken from different aquatic compartments, including surface water and sediments from the marine and freshwater environment, waste water effluents, and freshwater organisms. Data were obtained using state-of-the-art FTIR-imaging, using the same automated imaging post-processing software. We introduce a workflow with two quality criteria that assure minimum data quality loss due to volumetric and filter area subsampling. We find that probability density functions (PDFs) for particle length follow power law distributions, with median slopes ranging from 2.2 for marine surface water to 3.1 for biota samples, and that these slopes were compartment-specific. Polymer-specific PDFs for particle length demonstrated significant differences in slopes among polymers, hinting at polymer specific sources, removal or fragmentation processes. Furthermore, we provide PDFs for particle width, width to length ratio, area, specific surface area, volume and mass distributions and propose how these can represent the full diversity of toxicologically relevant dose metrics required for the assessment of microplastic risks.

1. Introduction

Environmental microplastic consists of a complex, diverse mixture of particles with different sizes, shapes and polymer types (Burns and Boxall, 2018; Kooi and Koelmans, 2019; Rochman et al., 2019). Discrete classifications of these properties are however unable to capture the full diversity of the microplastic mixture (Kooi and Koelmans, 2019). Better parameterization of this mixture is needed, for those seeking realistic risk assessments (Everaert et al., 2020; Koelmans et al., 2020). Probability density functions (PDFs) are mathematical functions that describe the actual distribution of a certain microplastic characteristic. As such they have the potential to capture the continuous nature of the different properties of these diverse mixtures (Kooi and Koelmans, 2019).

The advantage of these PDFs as opposed to more traditional discrete binning or classification methods is the level of detail that is maintained when presenting the results. Distributions can be compared more easily since their presentation is independent of the chosen bin width or class. Additionally, when the PDFs are parameterized, the resulting functions can form the basis for probabilistic (risk) modeling (de Ruijter et al., 2020; Kooi and Koelmans, 2019; Mohamed Nor et al., 2021). They allow for the accurate definition of the dose metrics that are relevant for ecological effects or toxicological effects on humans, while retaining the diversity of environmental or dietary microplastic. For risk characterization, these dose metrics can be aligned for the exposure and effect assessment, by taking into account the effect mechanism (Koelmans et al., 2017). Thus far, PDFs have been parametrized for microplastic sizes, shapes and densities (Kooi and Koelmans, 2019), and these parameters have been used for risk assessments in the marine and freshwater environment (Everaert et al., 2020; Koelmans et al., 2020). A similar probabilistic approach has been used to characterize microplastics in food and air, resulting in a probabilistic exposure assessment for humans (Mohamed Nor et al., 2021).

The parameterization by Kooi and Koelmans (2019) was based on best available information, however, data on individual particle

* Corresponding author.
E-mail address: merel.kooi@wur.nl (M. Kooi).

https://doi.org/10.1016/j.watres.2021.117429
Received 10 April 2021; Received in revised form 2 July 2021; Accepted 8 July 2021
Available online 14 July 2021
0043-1354/© 2021 The Author(s). Published by Elsevier Ltd. This is an open access article under the CC BY license (http://creativecommons.org/licenses/by/4.0/).

characteristics was not available. Empirical data on particle size was obtained from published tables and graphs, so only binned count data for (arbitrary) size classes was used. Despite being a commonly used method, fitting a power law on binned data via linear regression on the log-log scale can result in substantial biases of the parameter estimates because with binning one loses the information on trends in the data within a bin (Clauset et al., 2009; Newman, 2005; White et al., 2008). A better approach is the maximum likelihood estimation (MLE) method (Clauset et al., 2009; Newman, 2005; White et al., 2008). For particle shape and density, Kooi and Koelmans (2019) combined average relative abundances of shape categories and polymer types with estimates of 3D shape descriptions and polymer densities. These also are less accurate than actual data on shape and polymer ID on an individual particle level. Therefore, here we aim to provide parameterizations of microplastic PDFs, this time based on much higher-quality datasets with characteristics on the individual microplastic particle level.

Microplastic characteristics such as size, shape and polymer type, can be obtained on the individual particle level using Fourier transform infrared (FTIR) imaging or Raman microspectroscopy, or when combing visual selection with attenuated total reflection (ATR)-FTIR. When combining FTIR imaging with automated analyses software like siMPle and the MPAPP (Primpke et al., 2020a, 2019), the comparability between studies is greatly enhanced. However, this type of detailed analyses, and the required sample preparation, is very time-consuming. Therefore, most researchers analyze only a fraction of their sample and filter, and assume that results obtained for these subsamples would apply to the whole sample and thus can be extrapolated back to 100% sample size (Lorenz et al., 2019; Mintenig et al., 2020). Although this is a common approach, few studies assessed to what extent subsampling affects the assessment of particle property distributions (Abel et al., 2021; Brandt et al., 2021). Consequently, before detailed analyses of the actual data can take place, a better understanding of the adequacy of sample extrapolation is required.

Aim of the present paper is to provide characteristics of microplastic particles across environmental compartments, via continuous distributions. Secondary aims are to assess to what extent subsampling affects the accuracy of such distributions, and to discuss how these distributions can be used to tackle the multidimensionality of microplastic with respect to dose metrics as used in risk assessment for the environment and human health. We perform a meta-analysis of data from five studies that used state-of-the-art FTIR imaging and automated image analyses software (Lorenz et al., 2019; Mani et al., 2019; Mintenig et al., 2020; Pan et al., 2021; Primpke et al., 2019). First, we quantify the loss of accuracy in PDF quantification due to subsample extrapolation, and set two quality criteria to assure representativeness. The five studies focused on different aquatic compartments, i.e. freshwater, marine surface water and sediment, waste water effluent and freshwater benthic invertebrates. We present and compare PDFs for microplastic length, width, width to length ratio, area, specific surface area, volume and mass, for the different aquatic compartments. Additionally, we parameterize and compare power law distributions (using the MLE-method), focusing on the aquatic compartment level, the sample level, and the polymer level. The distributions are discussed in the context of a realistic risk assessment framework capable of accommodating all microplastic dose metrics that may be relevant given the effect mechanisms identified for particulate matter from the environment (de Ruijter et al., 2020; Kögel et al., 2020; Wright and Kelly, 2017).

2. Methods

2.1. Data collection

Particle length, width and polymer type data from five studies targeting different environmental compartments were used. The environmental compartments include marine surface water and sediment (Lorenz et al., 2019), freshwater surface water (Mintenig et al., 2020), freshwater sediment (Mani et al., 2019; Pan et al., 2021), waste water effluent (Mintenig et al., 2020; Primpke et al., 2019) and benthic freshwater biota (Pan et al., 2021) (Fig. 1). Note that results we obtain are specific for these datasets and do not necessarily apply to all sediment, water or biota samples worldwide.

The studies differed regarding sampling methods and examined sample type (Table S1) but are comparable analytically. Particles >500 μm (Lorenz et al., 2019; Mani et al., 2019) or >300 μm (Mintenig et al., 2020; Pan et al., 2021) have been analyzed using stereo-microscopes and ATR-FTIR analysis. No data on particles >500 μm were available for the German waste water effluents (Primpke et al., 2019). Smaller particles were analyzed using μFTIR. Instruments from different manufacturers were used that either applied a focal plane array (FPA) detector (Bruker Hyperion 3000 (Lorenz et al., 2019; Mani et al., 2019; Primpke et al., 2019), Agilent Cary 620 (Pan et al., 2021)) or a single element detector (ThermoFischer Scientific Nicolet iN10 (Mintenig et al., 2020)). Further, all FTIR data were analyzed using the same reference database (Primpke et al., 2018) and automated particle identification using the software siMPle and MPAPP (Primpke et al., 2020a, 2019). The lower size detection limit depended on the μFTIR instrument and settings used, and was either 11 μm (Lorenz et al., 2019; Mani et al., 2019; Primpke et al., 2019) or 20 μm (Mintenig et al., 2020; Pan et al., 2021).

Image analysis provided information on the particle's length, width and polymer type. Based on these variables, other particle properties, including width to length ratio (W:L), surface area, volume, mass and specific surface area (SSA), were calculated. Particles were assumed to have an ellipsoid shape for surface area and volume calculations (Koelmans et al., 2020; Primpke et al., 2020b; Simon et al., 2018). Since the height of particles cannot be measured using ATR-FTIR and μFTIR imaging techniques, it was assumed that the median W:L ratio is equal to the median height to width ratio; therefore the height was calculated as median W:L ratio times width (Koelmans et al., 2020; Kooi and Koelmans, 2019; Primpke et al., 2020b; Simon et al., 2018). Particle mass was estimated by multiplying particle volume with the density of the detected polymer (Table S2). Specific surface area was calculated as the surface area divided by the mass.

2.2. Extrapolation of subsample analyses

Most studies analyze only a part of their samples and/or filter areas, after which data are extrapolated to represent the full sample. This assumes particle characteristics detected for the subsample would apply to the whole sample as well. Since in reality two microplastic particles are never identical, this is a critical assumption. Using simulated samples and particles we tested to what extent subsampling and subsequent extrapolation influences the parameters of PDFs for particle size. Subsequently, we set two quality criteria, based on the minimum number of particles in a sample (criterium 1) and the subsample percentage of the sample or filter (criterium 2) to assure we adequately capture the size distribution of a full sample. In order to be able to include a sample in the further data analyzes, at least one of the criteria had to be met. For details on these tests, the reader is referred to the Supporting Information (Section S1). After this quality screening the number of particles included for each of the compartments was 3890 (biota samples), 10,356 (effluent), 19,676 (freshwater sediment), 1748 (marine sediment), 21,004 (freshwater surface water) and 2502 (marine surface water).

2.3. Parameterization of probability density functions

Cumulative frequency distributions (CFDs) were plotted for particle length, width, W:L ratio, area, volume, mass and specific surface area, as well as relative abundances of polymer types per environmental compartment. Median and mean values, quantile ranges and standard deviations for these different properties were calculated. Subsequently, probability density functions (PDFs) were fitted for particle length,

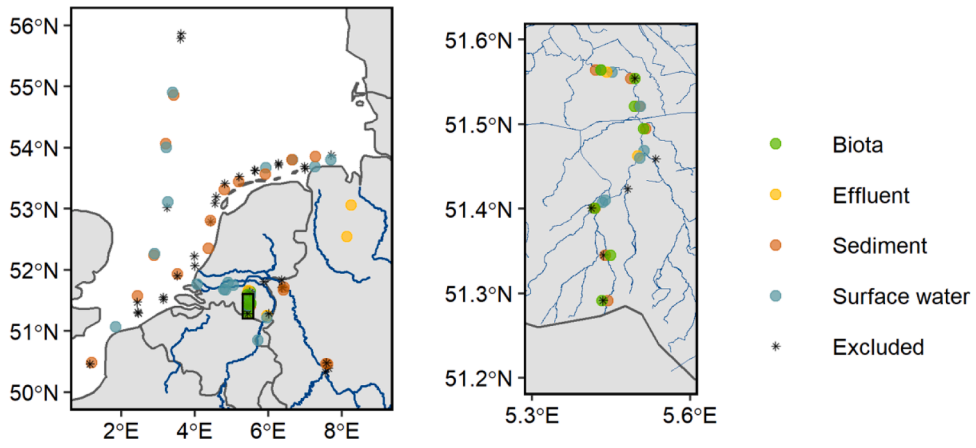

Fig. 1. Map of the sample locations, with colors indicating the different aquatic compartments. The detailed map is a cutout of the river Dommel, where many different samples have been taken in the main tributary. Points are slightly dodged to avoid overlap. Black stars indicate samples that did not meet the quality criteria (see Sections 2.2 and 3.1) or did not contain plastic particles, and were therefore excluded from further analyses.

width, area, volume and mass, for the six compartments. PDFs for length and width were also analyzed on the sample level, and for length also on the polymer level. The particle length distribution of microplastics has been shown to follow a power law shape (Eq. S1) (Kaandorp et al., 2021; Kooi and Koelmans, 2019; Mattsson et al., 2021), and the same can be expected for width. Since particle height was calculated using the median W:L ratio times the width, particle height will also follow a power law profile. If particles would be perfect spheres or squares, one would expect a power law slope for volume of one third of the slope of length. Our particles are assumed to be ellipsoid-shaped, so we expect the volume and surface area to follow a power law as well, however with a lower slope exponent compared to the ones for length and width. Given the large range in volumes (several orders of magnitude) and the relatively small range in densities, particle mass is expected to also follow a power law distribution, with a similar slope as the one for particle volume. The reciprocal of specific surface area, calculated as surface area divided by mass, was found to also follow a power law distribution after visual inspection of histograms.

2.3.1. Fitting power laws

Power laws usually only apply to values greater than some minimum (x_{min}), in our case the minimum particle length, width, area, volume or mass. This minimum size was determined using Kolmogorov-Smirnov (KS) statistics (Clauset et al., 2009). The maximum distance between the cumulative frequency distributions of the data and the model for a combination of x_{min} and α was determined. This calculation was optimized to minimize the difference between the two distributions, resulting in the optimal $\widehat{x}_{min}$. The power law exponent α was then estimated as $\widehat{\alpha} = 1 + n\left[\ln\sum_i \frac{x_i}{\widehat{x}_{min}}\right]^{-1}$, according to maximum likelihood estimation (MLE) method (Clauset et al., 2009; Newman, 2005). To ensure good parameter estimates, each fit was bootstrapped, to obtain means and standard deviations of both $\widehat{x}_{min}$ and $\widehat{\alpha}$. Calculations were performed with the poweRlaw package (Gillespie, 2014). The estimation method was applied on three different levels: (a) the compartment level, (b) the sample level, and (c) a lumped aquatic system level.

2.3.2. Particle distributions per aquatic compartment

To obtain average distributions for particle length, width, area, volume and mass per aquatic compartment, we applied the MLE method on the datasets that were extrapolated to have an identical sample volume (Section 2.2). Particles >5000 μm in length were excluded from the analysis since a portion of these particles were removed by sieves before the analyses, but some slipped through. Therefore, it is unknown what fraction of all >5000 um particles was actually analysed. With a bootstrap ($n = 100$), the mean and standard deviation of both $\widehat{x}_{min}$ and $\widehat{\alpha}$ were determined.

Additionally, for particle length and width, we calculated $\widehat{x}_{min}$ and $\widehat{\alpha}$ for each sample individually, again only for particles ≤5000 μm in length. For some samples, only one or two unique particle sizes were reported. These samples were excluded from power law fitting, given the lack of (continuous) distribution data. Also, we set a threshold of at least 10 particles for a sample to be included. A final criterion was that the estimated mean $\widehat{\alpha}$ had to exceed two times the standard deviation of $\widehat{\alpha}$, based on bootstrapping ($n = 500$). Having one power law exponent per sample, we calculated median slopes per aquatic compartment.

An 'average' power law exponent for aquatic microplastic was calculated by combining data for the four relevant aquatic compartments, i.e. surface waters and sediments in both the marine and freshwater environment. Since the number of samples differed per aquatic compartment, a random subset of 5 exponents per compartment was selected, and the mean of these 20 exponent values was calculated. To account for the random variability, this process was bootstrapped ($n =$ 10,000). Based on these results, one overall power law exponent for aquatic microplastic length and width was obtained.

2.3.3. Particle size distributions per polymer type

Besides calculating power law exponents per sample, we calculated exponents per polymer type per sample, for particle length only. Here, the same quality criteria as for the sample level calculations applied, i.e. ≥2 unique sizes, ≥10 individual particles, and the bootstrapped ($n =$ 500) mean was required to exceed two times the standard deviation. We compared exponent distributions per polymer type, and tested if correlations between exponents of different polymer types across samples occur (Spearman's rank correlation test).

2.3.4. Comparison of the particle size distributions

We tested for significant differences in power law exponent distributions between the different aquatic media or polymer types using a non-parametric Kruskal-Wallis rank sum test, followed by a pairwise Wilcoxon rank sum test, with a significance threshold of $p = 0.05$.

Additionally, Spearman's rank correlation coefficients were calculated for the polymer-specific power law exponents. Spearman's correlation provides a pairwise comparison on the sample level, between two polymers, contrary to Kruskal-Wallis and pairwise Wilcoxon rank sum tests, that test for differences between groups. The Spearman's correlation coefficient would be 1 or −1 if the two polymers show a monotonic relationship, that is, if the exponent of one polymer in a certain sample would increase or decrease, so would the exponent of the other

polymer in the same sample.

3. Results and discussion

3.1. Selection of representative samples based on extrapolating

An analysis was performed to verify to what extent subsampling negatively affects the representativeness of power law slopes obtained from extrapolated datasets. Based on the comparison of the fitted linear regression with the 1:1 lines, we conclude that original datasets with ≥500 observations are acceptable (Figures S1, S2). Similar to the particle number criterium, we also checked for the representativeness of subsample percentages of the sample or filter. Here, based on comparison of original versus extrapolated alpha values inferred from our simulated datasets, we set the criterium threshold at 60% (Figures S3, S4). Therefore, after extrapolation based on the correction factor (CF), we excluded datasets with both <500 particles *and* <60% of the sample or filter analyzed, from further analyses.

Note that our 60% criterium, meant for finding accurate power law slopes, is consistent with two, laboratory based, criteria, where it was recommended to analyze at least 50% of the filter (Brandt et al., 2021; Mintenig et al., 2020). What both the theoretical and lab-based approach did not take into account was the sample volume. For instance, a large sample analyzed for 40% might give a better representation of the actual environmental composition than a small sample analyzed for 80%. After all, for the estimation of a power law exponent for a sample we need a sufficient number of particles, irrespective of the volume of that sample. Sample volume criteria for natural waters have been suggested (Koelmans et al., 2019), however these are independent of subsample percentages. Ideally, there would be a combined criterium, based on expected plastic concentrations, sample volume and subsample percentages.

With these two criteria in effect, 39 out of the 129 samples were excluded from our analyses (Fig. 1, black stars, Table S1), while the remaining 90 samples were composed of 9 marine surface samples, 13 marine sediment samples, 21 freshwater surface waters, 11 freshwater

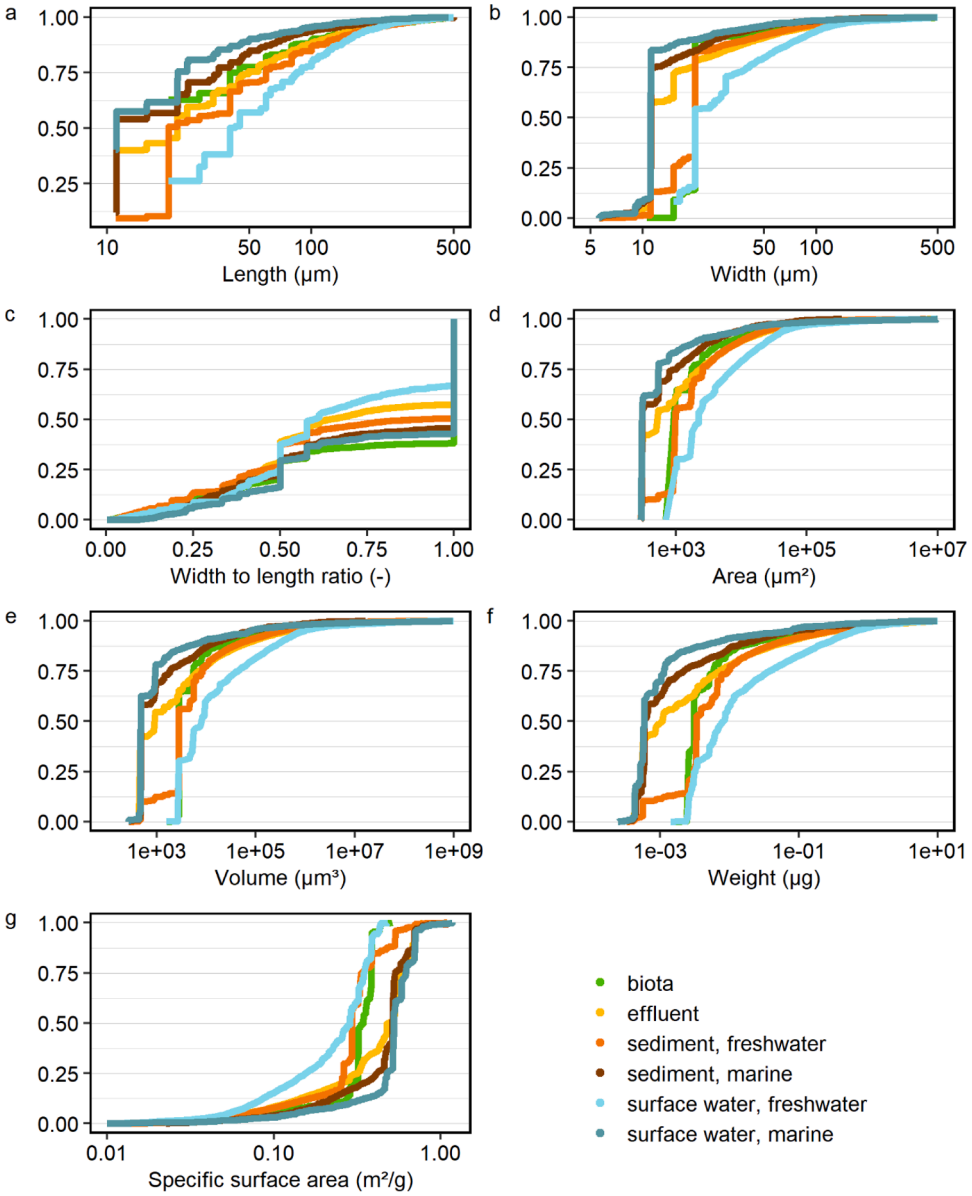

Fig. 2. Cumulative frequency distributions for microplastic properties per particle, with a) length, b) width, c) width to length ratio, d) area, e) volume, f) weight and g) specific surface area. All distributions are plotted on a log x-axis scale, except for panel c, which uses a linear x-axis scale. The different colors indicate the different aquatic media.

sediments, 8 effluent samples and 28 biota samples.

3.2. Characteristics of aquatic microplastics

Cumulative distribution functions (CDFs) for particle length, width, width to length (W:L) ratio, surface area, volume, mass, and specific surface area capture the multidimensionality of microplastic characteristics (Fig. 2; Table S3). Here we discuss the main features of these distributions, while later on we illustrate how they can inform the risk characterization based on specific effect mechanisms that require the specific data from these distributions (Section 3.6). Particle length has some clear discrete steps, which is the result of the pixel-based analyses when using μFTIR (Primpke et al., 2020b) (Fig. 2a). It is also clear that biota and freshwater surface water samples were analyzed with a detection limit of 20 μm as compared to 11 μm for the other samples. Freshwater sediment samples have been analyzed using two μFTIR instruments and with different settings, which explains the rapid rise at 20 μm. Although the upper size limit of the samples is around 5000 μm, and even larger for some fibers, almost all the particles are <300 μm in length. At least 25% of the particles have a length equal to the detection limit (Table S3, first quantile), and for biota, freshwater surface water, freshwater sediment and marine sediment, the median is also very close or equal to the detection limit (Table S3). This illustrates the need for detailed analyses, where samples taken with meshes of 300 or 500 μm will not suffice to get representative plastic concentrations. Benthic invertebrate samples contained the largest portion of small particles, where a length larger than 20 μm occurs for less than 40% of the particles. We assume this is the result of size-selective feeding, where ingestion is limited by the mouth-opening of the organisms (Bern, 1990; Jâms et al., 2020; Koelmans et al., 2020).

Fibers and particles have been combined in all of the analyses in this study. Here, we defined fibers as particles that have a length to width ratio ≥ 3, and a diameter of 15 μm (Mintenig et al., 2020; Primpke et al., 2019). For all samples, 7.4% of the particles are classified as fibers. In the marine environment, hardly any fibers are found, with percentages <0.1%. For effluents, this percentage is 7.0%, for biota 8.6%, for freshwater surface waters 9.2% and for freshwater sediments 13.4%. The minimum length for fibers for the four compartments where fibers are abundant is 60 μm. Median lengths range from 100 to 140 μm, and maximum values vary between 2060 and 7470 μm.

Even more so than for length, the width of at least half of the particles is 11 or 20 μm (Table S3). For biota, freshwater surface water, freshwater sediment and marine sediment, even the upper quantile is very close to the detection limit; indicating that 75% of the data has a width of 20 or 11 μm. The width is calculated based on the pixel arrangement (Primpke et al., 2020b, 2019), and can therefore be smaller than the detection limit. Because of this interpolation, the CDF is more smooth as compared to the CDF for particle length.

The W:L ratio has a clear dominance of 1, i.e. the width is equal to the length. This can be explained by the dominance of small particles combined with the pixel-based analyses. Around 25% of the particles have a W:L ratio ≤ 0.5 (Fig. 2c, Table S3). The median W:L ratio is 0.67 for all particles, including fibers, which was used to calculate the particle height and subsequently the volume. This value is close to the values used in the MPAPP (0.7) and by Simon et al. (0.69), which are both mean values of a smaller dataset (Primpke et al., 2020b; Simon et al., 2018). The mean value for all our particles is 0.69 too, however, since the data are not normally distributed, the median value was used for further calculations.

Particle area, volume and weight show rather continuous distributions (Fig. 2d, 2e, 2f), still with rapid increases for the lower particle sizes. Particle volume and mass range over several orders of magnitude, which is the result of the three-dimensional shape of particles that already varies two orders of magnitude in length and width. Specific surface area (Fig. 2g) shows a rapid increase only for the larger values, seemingly the inverse of the other distributions, which makes sense given it was calculated as surface area divided by weight. Median values for the SSA range from 0.29 $m^2\ g^{-1}$ for freshwater surface waters to 0.53 $m^2\ g^{-1}$ for marine surface waters (Table S3). These values are in the same order of magnitude as SSA values reported for different microplastic polymers; those ranged between 0.59 and 3.2 $m^2\ g^{-1}$ (Godoy et al., 2019).

Whereas particle mass is mainly influenced by the large variability in particle volumes, polymer densities are all relatively comparable (Table S2, Table S3). However, relative abundances of these different polymer types are different for different aquatic compartments (Fig. 3). The largest percentage of buoyant polymers is found in freshwater surface waters, followed by effluents, benthic biota and marine surface waters. Sediments have the lowest percentage of buoyant polymers, which makes sense given that particles need to settle from the water column in order to reach the sediment. Processes like aggregation and biofouling can result in the settling of buoyant plastics to the sediment layer, however, these processes take time (Kooi et al., 2018). Effluents and freshwater sediments show the highest abundance of acrylates; potentially most of these particles settle in river sediments before they reach the marine environment. On the other hand, polyamide and polychloroprene are mainly found in the marine environment, so they could originate from another source than terrestrial inputs. For fibers, the polymer composition in the four compartments that contained substantial amounts (i.e. biota, effluents and the freshwater compartments) differed little from the overall sample analyses, with acrylates still the most abundant in freshwater sediments and rod-shaped rubber type 3 particles (mainly ethylene propylene diene monomer (EPDM) rubber) dominating the polymer distribution for biota.

Since all these distributions account for the actual multidimensionality of the particles, they represent a powerful tool set to assess the environmentally relevant exposure to biota.

3.3. Microplastic particle size distributions for aquatic compartments

Power law distributions were fitted on all data per water type, for particle length, width, area, volume and mass (Table S4, Figs. 4, S5 - S8). The minimum length for which the power law distributions are valid range from 56 ± 21 μm for marine sediment to 354 ± 86 μm for freshwater sediment (mean ± standard deviation). Below this minimum length, the observations start to deviate from the fitted distribution. Mean power law exponents for particle length range from 2.1 ± 0.03 for marine surface water to 3.3 ± 0.19 for freshwater sediment.

For particle width, exponent values were very comparable to the ones found for particle length, ranging between 1.96 ± 0.03 for marine surface waters to 2.87 ± 0.17 for freshwater sediments. Since many of the particles have a W:L ratio of 1 (Fig. 2c), this was expected. The minimum size for which the width distributions follow a power law distribution are somewhat lower, between 22 and 127 μm (Table S4, Figure S5).

For particle area, exponents are 1.3 – 1.7 times lower than for length, with exponents ranging between 1.50 ± 0.009 for marine surface waters and 2.00 ± 0.065 for freshwater surface waters (Fig. S6). For particle volume, exponents were again lower compared to particle length. For perfect spherical particles, a three times lower exponent would be expected for volume compared to length. Given the ellipsoid-shaped particles, the decrease was expected to be less than that, so the 1.4 – 2.1 times lower exponent values for volume compared to length seem reasonable. For particle volume, power law exponents ranged between 1.40 ± 0.004 for biota and 1.68 ± 0.08 for freshwater surface water (Fig. S7). As expected, exponents for particle mass differed little from those for volume, with values ranging between 1.32 ± 0.01 for marine surface waters and 1.65 ± 0.07 for freshwater surface waters (Fig. S8). The specific surface area (SSA) distributions per environmental compartment were parameterized as the reciprocal of SSA (Fig. S9, Table S4). The mean exponent values range between 1.98 ± 0.30 (marine surface water) and 2.82 ± 0.10 (freshwater sediment).

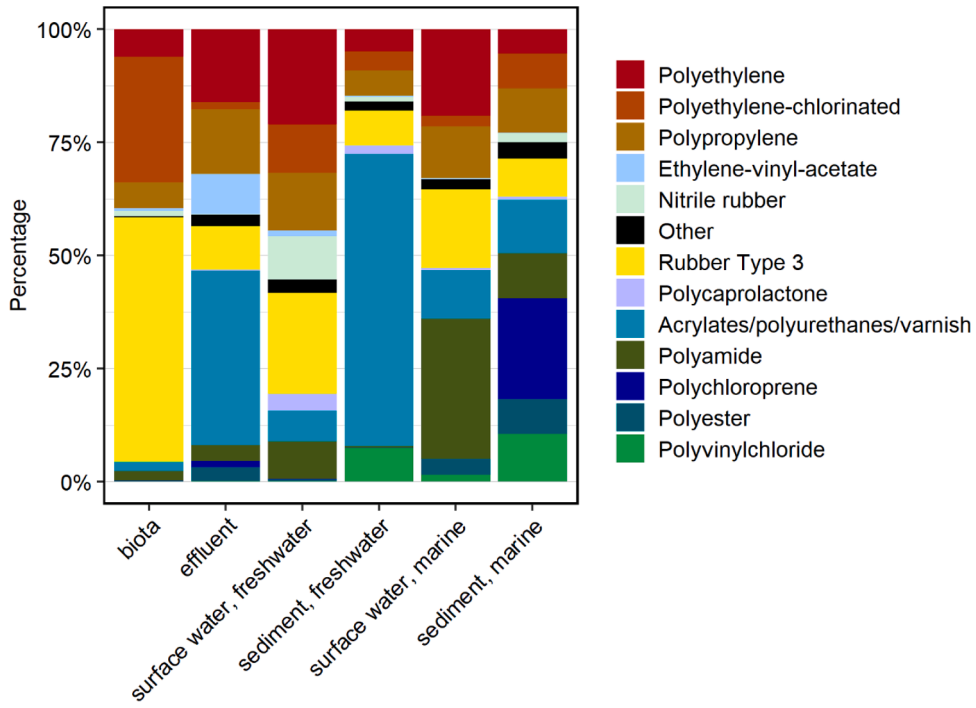

Fig. 3. Relative abundance of different polymers per aquatic compartment. Polymer types were labeled as "Other" when their abundance was <2% in all of the compartments. Polymers are ordered based on their density (Table S2), with all buoyant polymers above the "Other", and all non-buoyant ones below, assuming a density threshold of 1 g cm^{-3}. "Other" polymers constitute a mixture of densities.

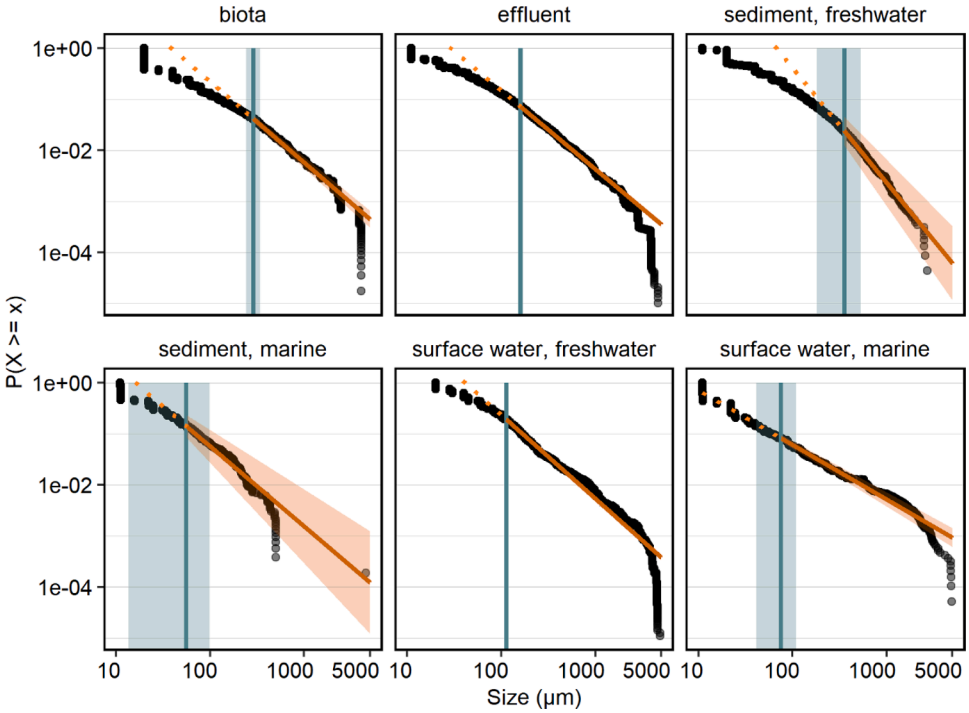

Fig. 4. Particle length distributions for the different compartments. The blue vertical segments indicate the minimum size for which the fitted power law is valid. The brown slopes present the fitted power law distributions. The mean (solid line) and standard deviation (shaded area) are based on $n = 100$ bootstraps. The dotted line shows the continuation of the fitted slope beyond the minimum size. Here, the deviation of the particles from this line is apparent. Mean exponent parameters are 2.59 ± 0.04 for biota, 2.54 ± 0.01 for effluent, 3.25 ± 0.19 for freshwater sediment, 2.57 ± 0.20 for marine sediment, 2.64 ± 0.01 for freshwater surface water and 2.07 ± 0.03 for marine surface waters (Table S4).

What should be noted for all these distributions, is that the fitted minimum size and exponent are not independent. In general, the exponent increases with increasing values of the minimum size. For the presentation of the data, we assumed independence, with the mean value for the minimum size as starting point of the valid fitted power law domain (Figs. 4, S5 – S9). For the largest particles, the power law distribution tends to overestimate the actual abundance. However, there are very few of these larger particles in the samples compared to the number of particles in the size ranges for which the power law is most accurate.

To further study the variability in particle size distributions, power law distributions for particle length and width were fitted for individual samples (Fig. 5). For length, the estimated values for the minimum length for which the power law is valid ranged from 20 to 832 µm, for the 68 datasets that met the quality criteria (Section 2.3.2). The exponents ranged from 1.4 to 7.9 for all samples. The power law exponent

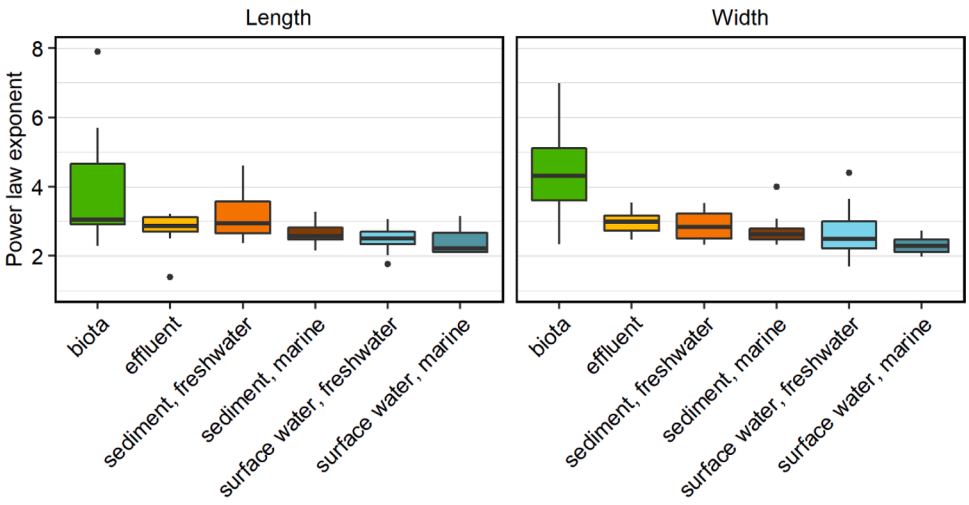

Fig. 5. Power law exponent distributions for the different media, for particle length (left) and width (right). Median exponents for particle length are 3.05 ($n = 12$) for biota, 2.86 ($n = 8$) for effluent, 2.94 ($n = 11$) for freshwater sediment, 2.58 ($n = 11$) for marine sediment, 2.5 ($n = 20$) for freshwater surface water and 2.2 ($n = 6$) for marine surface water. For particle width, median exponents are 4.31 ($n = 8$) for biota, 2.98 ($n = 8$) for effluent, 2.83 ($n = 10$) for freshwater sediment, 2.61 ($n = 12$) for marine sediment, 2.49 ($n = 21$) for freshwater surface water and 2.29 ($n = 5$) for marine surface water.

distributions for particle length of most compartments did not differ significantly from one another ($p > 0.05$). Only freshwater surface water differed significantly, both from biota ($p = 0.0056$) and from freshwater sediment ($p = 0.042$).

For particle width, 64 datasets were included after taking into account the quality criteria. Minimum values for which the power law is valid ranged from 12 to 511 μm, and power law exponents ranged from 1.7 to 7.0 for all samples. For width, only freshwater surface water and biota differed significantly ($p = 0.034$). There were no significant differences between the exponents for particle length and width, when performing a pairwise comparison per environmental compartment.

Besides the median values and ranges for the different compartments, we also calculated one average 'aquatic microplastic' power law slope based on the four aquatic compartments, i.e. marine and freshwater sediment and surface water. We found that the length distribution of aquatic microplastic can best be described using a power law with a slope of 2.68, with values for individual samples ranging between 1.76 and 4.62 (Fig. 5). For width, the best estimate for the slope is 2.64.

3.4. Microplastic particle size distributions per polymer type

Particle size distributions were calculated per polymer type, per sample (Fig. 6). In total, 421 power law exponents were calculated that fulfilled the set thresholds (Section 2.3.3), for a total of 21 different polymer types. Comparison of the exponents for different polymer types, irrespective of environmental compartment, revealed significant differences between both polyethylene (PE) and polypropylene (PP) with acrylates, polyamide, polyethylene-chlorinated and rubber type 3 ($p < 0.05$). PE also differed significantly with nitrile rubber. Median values of the power law exponents for PE (2.5) and PP (2.7) are low compared to those for these other polymers, i.e. rubber type 3 (3.0), nitrile rubber (3.1), acrylates (3.2), polyamide (3.2), and polyethylene-chlorinated (3.3). This implies that relatively many large PE and PP particles are present in the samples, compared to the other polymers.

There are several mechanisms that could explain the observed differences in polymer-specific size distributions: different entry size of polymer particles, polymer-specific removal processes and fragmentation kinetics. The density of PE and PP is lower than the density of most of the other polymers (Table S2), and lower than that of water. At the same time, water samples are most abundant in our dataset (Fig. 5,

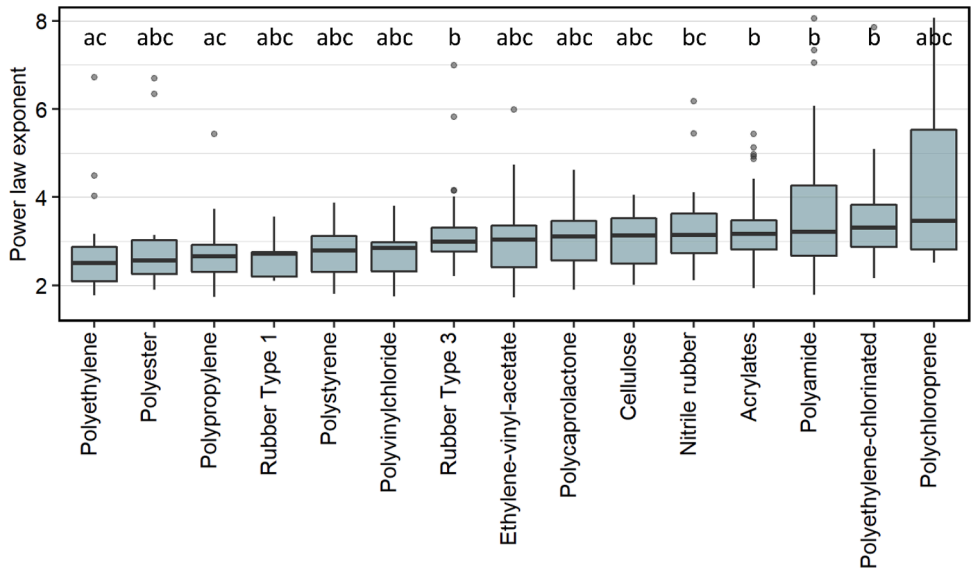

Fig. 6. Power law exponents for different polymers ordered in increasing median power law exponent. Here, at least 5 individual exponent estimates are included per boxplot. With pairwise comparison, polyethylene and polypropylene were found to have a significantly lower median value compared to acrylates, polyamide, polyethylene-chlorinated and rubber type 3. Polyethylene also differed significantly with nitrile rubber. Cellulose refers to chemically modified cellulose.

Table S1). It is possible that size-selective settling of larger particles occurs for the non-buoyant plastics, i.e. acrylates, polyamide, rubber type 3 and nitrile rubber. With preferential removal of larger particles from the water surface, the power law exponent values will increase. Further, differences in fragmentation kinetics, i.e. resistance to fragmentation, could also affect the size distributions of different polymer types. Fragmentation is driven by environmental factors, including UV radiation, wind, waves and biodegradation, and the rate of fragmentation depends on physical, thermal and mechanical properties of the polymer (Min et al., 2020). Little is known about actual fragmentation rates, but polymers have been ranked on their probability of surface erosion, with that probability increasing with decreasing hydrophobicity. Polyethylene and polypropylene have a low probability of surface erosion, whereas polyamide and acrylates are more likely to experience surface erosion (Min et al., 2020). Therefore, all of these mechanisms provide plausible explanations for the observed polymer-specific size distributions.

The groupwise comparison among polymers indicates polymer-specific particle size characteristics. Aside from this groupwise comparison, we also tested for rank correlations (i.e. Spearman's rank correlation test). With these correlations, the focus is on the pairwise comparison on the sample level, in other words, are there differences in particle size characteristics between different sample locations? We found significant correlations ($p < 0.05$) for 9 polymer pairs, with correlation coefficients varying between −0.7 and +0.9 (Table S5, Fig. S10). For these polymers, it is clear that size distributions are location dependent, that is, some samples have relatively more small particles for the two correlated polymers compared to other samples. It is possible that differences in sources, environmental conditions that influence aggregation and biofouling, and physical processes that influence settling and burial explain the differences between the different locations. Environmental compartments alone do not seem to explain the difference in exponent values for different samples (Fig. S10).

Some polymers that did not differ significantly in the group-wise comparison, do show a significant correlation. With comparison on the polymer level, a large spread in exponent-values will likely cause the polymer to *not* differ significantly from other polymers. On the other hand, such a large spread can still result in significant correlations, as long as the values are paired per sample location.

3.5. General applicability of exponent values

The compartments that we studied were heterogeneous. For instance, rivers in itself already represent a wide range of turbulence conditions. Furthermore, the studied compartments contained subsets from different systems, e.g. sediment from Rhine and Dommel, surface water from Meuse, Dommel and ditches adjacent to the Dommel, implying that different sediment morphologies and hydrodynamics are included. Nevertheless, our data shows that the exponent values calibrated per compartment have low relative standard deviation (Table S4). We argue that the exponent values, although operationally defined, can be used in a generic way for similar compartments. However, we emphasize that it would still be best if scientists studying other environmental systems or areas use the workflow presented here to obtain system-specific PDFs and exponent values. Exponent values calibrated for a specific compartment and set of conditions will always be most accurate. Only if such data are not available, the exponent values provided here could be considered as best available proxies for other systems. The values must then be used taking into account the uncertainty, for example by probabilistic modeling using a range of exponent values. We recommend this would anyway always be done when using the average value of 2.68 for aquatic microplastic.

Another aspect related to applicability is the extent to which power law distributions and exponent values could make sense beyond the upper and lower bounds. A recent study parameterized a theoretical particle length distributions for ocean surface waters, based on a cascading fragmentation model and taking into account different, size-selective, particle transport processes (Kaandorp et al., 2021). Although model assumptions differed from some of the environmental conditions in the present dataset, they report a power law exponent value of 2.67 based on fractal fragmentation alone, which is similar to the average exponent value of 2.68 that we found for aquatic microplastic, i.e. when combining freshwater and marine surface waters and sediments. The minimum size for which their power law regime was valid was in the order of several millimeters, whereas in our study minimum sizes ranged from 50 to 350 μm. This agreement may suggest a wider applicability; above our present upper size limit. In contrast, at the lower end of the size range, a study of nano-fragmentation of expanded polystyrene in a closed and mixed system showed that particle size distributions followed a power law shape distribution from 5000 down to 0.1 μm (Mattsson et al., 2021).

The lower than expected abundance of the smallest particles based on the power law prediction (Fig. 4) can be explained by size-selective processes such as wind mixing, aggregation, settling and beaching (Kaandorp et al., 2021; Kooi et al., 2018). However, since we do not find a higher abundance of these smallest particles in sediments, only aggregation and consequent settling would not explain this deviation from the power law regime. Another potential explanation relates to detection accuracy: Mattsson et al. could detect particles down to 10 nm by combining three different instrumental analytical techniques each targeting a part of the total size range (Mattsson et al., 2021), whereas in our study detection limits were 11 or 20 μm, depending on the μFTIR instrument used. In the theoretical fragmentation study, data used for calibration reported values down to 100 μm (Kaandorp et al., 2021). So it seems that with a lower size detection limit, the minimum size for which the power law regime is valid is also lower.

An upper size limit for the power law regime is not clearly defined. The five studies used here aimed at quantifying small particles, and consequently could not always take very large sample volumes. Studies that focused on larger particles, e.g. >300 or 500 μm using trawls, found power law regimes to extend to larger particle sizes too (Cózar et al., 2014; Kaandorp et al., 2021). Similar to the minimum size, the maximum size for which the power law regime is valid might mainly be a result of sampling design.

We therefore argue that the presented power law exponents are likely to be valid from 1 to 5000 μm, that is, the whole microplastic size range, although further research to validate this is recommended especially for the low end of the size range. It is possible that distributions beyond those limits still follow the same regime, but since there is little data on this, it is difficult to verify at this moment. The here presented observations support published approaches that use power law extrapolations to rescale number concentration data obtained with methods that target only part of the microplastic size range, to the full 1 to 5000 μm size range (Everaert et al., 2020; Koelmans et al., 2020; Mohamed Nor et al., 2021).

3.6. Linking probability density functions to ecologically relevant dose metrics for risk assessment

We have discussed the main features of the probability density functions (PDFs) of different microplastic properties, for different compartments and polymers. All of these properties can inform risk characterization based on specific interactions with organisms that would require data specific to these distributions. Here, we discuss how these diverse interactions, their dose metrics, i.e. ecologically relevant metrics (ERM), and associated diverse microplastic characteristics can be unified to refine prospective risk assessment.

The distribution of particle length and width (Figs. 2a, 2b, 4 and S5) is relevant for quantifying bioavailability. Bioavailability can relate to size limits for tissue uptake or translocation (Mohamed Nor et al., 2021), or when for instance the mouth opening has to be larger than the width of the particle for ingestion to occur (Jâms et al., 2020; Koelmans et al.,

2020). The average power law slopes for aquatic microplastic length and width (Table S4) are much higher than the previously reported value of 1.6 (Kooi and Koelmans, 2019), which implies that the relative abundance of microplastics that is bioavailable to organisms is higher too.

The shape of the particle (Fig. 2c), here expressed via the width to length ratio, is important for shape-specific toxicity. Long, thin fibers for instance are considered more toxic (Au et al., 2015; de Ruijter et al., 2020; Gray and Weinstein, 2017; Ziajahromi et al., 2017). We have shown that fibers make up a significant part of the particles in our data set, so it is important to focus not only on the number of particles, but also on the shape.

Particle surface area is toxicologically relevant because it is the surface which makes contact with the biological system whereas the plastic itself is considered to have little toxicity. Surface area is considered to be the dose metric relevant for oxidative stress (Schmid and Stoeger, 2016). Furthermore, particle area is relevant for hazardous substances that bind to the surface: e.g. toxic trace metals and pathogens (Fubini, 1997; Schmid and Stoeger, 2016; Schwarze et al., 2007). Overall, particle surface area thus can be considered a very significant toxicologically relevant characteristic of small microplastic particles (Riediker et al., 2019), which emphasizes the importance of the environmentally relevant area distributions that now are available (Figs. 2d, S6).

Volume distributions (Figs. 2e, S7) would be required if one wants to quantify effects that depend on total volume ingested, such as the food dilution effect mechanism (de Ruijter et al., 2020; Rauchschwalbe et al., 2021), which can be used to correct species sensitivity distributions or other frameworks that target this effect mechanism (Koelmans et al., 2020).

Similarly, particle weight (Figs. 2f, S8) is relevant for effect mechanisms where the stressor needs to be expressed on a mass basis, like for organic chemical exposure, for which plastic associated-chemical concentrations are mass based (Bakir et al., 2016; Velzeboer et al., 2014). Mass distributions are also required for realistic number to mass conversions that remain true to the material as it occurs in nature (de Ruijter et al., 2020; Koelmans et al., 2020).

Some effect mechanisms for particle toxicity correlate best with specific surface area, i.e. area per mass ($m^2\ g^{-1}$) (Figs. 2g, S9). For instance, in vitro cytotoxicity (Guthrie Jr, 1997; Michel et al., 2014) and inflammation (Stoeger et al., 2006; Tran et al., 2000) are found to be related to the SSA of particles. Also, the SSA can be a measure for chemical adsorption to microplastics (Godoy et al., 2019).

Polymer type (Fig. 3) influences transport and fate characteristics of the particles, and therefore the bioavailability and accessibility for species living in different habitats. Besides bioavailability, biological and chemical interactions can also be polymer specific (Endo and Koelmans, 2016; Frère et al., 2018; Godoy et al., 2019; Velzeboer et al., 2014).

3.7. Alignment of exposure and thresholds effect concentrations for different dose metrics

For a consistent characterization of microplastic risk, the dose metric used for the exposure assessment needs to be the same as the metric used for the effect assessment (Koelmans et al., 2017). Because there are different exposure and dose metrics, we describe here a method to align and convert them. The example is based on number concentrations, however we provide equations to convert these into concentrations for other metrics as well. A numerical example for all calculations in this workflow is provided as Supporting Information (Section S3).

3.7.1. Rescaling exposure data

Previously we have provided a method to rescale environmental microplastic number concentrations measured with methods that target different size ranges, to the complete, default microplastic size range (i.e. 1 – 5000 μm) or any other desired size range (Koelmans et al., 2020). Given an upper limit (UL) and lower limit (LL) of the measured and default size range, a dimensionless correction factor (CF_{meas}) is defined that rescales the measured (M) number concentration for a certain size range to the number concentration for the microplastic default (D) size range (e.g., 1 to 5000 μm), based on the power law distribution for length (L) with slope α_L (Table S4) (Koelmans et al., 2020):

$$CF_{meas} = \frac{L_{UL,D}^{1-\alpha} - L_{LL,D}^{1-\alpha}}{L_{UL,M}^{1-\alpha} - L_{LL,M}^{1-\alpha}} \quad (1)$$

The measured exposure number concentration (C_{meas}; #/L) is multiplied with CF_{meas} to obtain a rescaled exposure number concentration ($C_{env} = CF_{meas} \times C_{meas}$) that represents the complete, environmentally relevant range. For best accuracy, a value for α_L is preferably used that is calibrated for the particular environmental compartment such as that in Table S4. The rationale for using compartment level exponent values (i.e. Table S4) is the ecological relevance for aquatic communities for which the habitat would be defined on a compartment level rather than a sample level.

Mean values such as those for 'aquatic microplastics' of 2.68 are better avoided unless the uncertainty around the mean is justified probabilistically.

3.7.2. Rescaling effect data

The rescaled exposure concentrations as calculated using Eq. (1) represent the default microplastic size range and should be compared to threshold effect concentrations (EC) for a particular effect mechanism (and thus ERM), which are expressed for the same default size range. This requires two corrections.

The first correction is needed because only a part of the default microplastic size range is bioavailable to exert effects. For instance, ingestion of the particles often is considered to be a prerequisite for particle effects (de Ruijter et al., 2020), in which case thus a correction for bioavailability via ingestion is required. Tissue uptake or translocation also are size restricted (e.g. Mohamed Nor et al., 2021), which thus also would require a size-related bioavailability correction. The required equation for these corrections is as follows. The threshold effect concentration for the bioavailable size fraction of particles (EC_{poly}; #/L) can be related to the threshold effect concentration for the environmentally relevant (1 to 5000 μm) range of particles (EC_{env}; #/L) by using a slight modification of the CF_{meas} in Eq. (1) (CF_{bio}):

$$EC_{env} = EC_{poly} \times CF_{bio} \quad (2)$$

The only difference between CF_{meas} and CF_{bio} is the use of UL,B and LL,B in the denominator for CF_{bio}, representing the upper and lower size limit of the bioavailable size fraction, respectively.

The second correction is required because reported effect concentrations almost always relate to *monodisperse* microplastic particles, whereas in nature, microplastic particles are *polydisperse*. This second correction is specific for the ERM under consideration, because polydispersity is defined by the power law slope for that ERM (Table S4). For a given effect threshold for ERM *x* (where *x* for instance is number, mass, volume, area or specific surface area) it does not matter if this threshold relates to mono- or polydisperse particles as long as the magnitude of the threshold remains the same (Koelmans et al., 2020). For instance, if the ERM is particle volume, one would calculate total volume of the monodisperse particles at the threshold effect number concentration reported in literature, and then calculate which number concentration of polydisperse particles has the same volume, while using the power law slope for volume (Koelmans et al., 2020). As this can be done for any ERM x, we here introduce a generic equation which preserves the ERM of interest between mono- and polydisperse particles at a certain ERM threshold effect level:

$$EC_{poly} \times \mu_{x,poly} = EC_{mono} \times \mu_{x,mono} \quad (3)$$

Here, EC_{mono} (#/L) is the effect number concentration for

monodisperse particles and $\mu_{x,\ mono}$ is the mean value for ERM x for these monodisperse particles (e.g., from literature test data). If the ERM is 'number', $\mu_{x,\ mono}$ is 1. Note that Eq. (3) can also be used to convert EC values for distributions with different degrees of polydispersity. If the probability distribution of ERM x follows a power law regime, the mean ERM value for the polydisperse particles, $\mu_{x,poly}$, can be calculated as:

$$\mu_{x,poly} = \frac{1-\alpha_x}{2-\alpha_x} \times \frac{x_{UL}^{2-\alpha_x} - x_{LL}^{2-\alpha_x}}{x_{UL}^{1-\alpha_x} - x_{LL}^{1-\alpha_x}} \tag{4}$$

UL and LL relate to the upper and lower limit in ERM x for which the mean is calculated, and α_x is the power law exponent value of ERM x. Note this equation does not apply when α_x is exactly 1 or 2; see section S2 for a derivation including versions for all α_x values, and Table S4 for different exponent values. Calculation of the limits UL and LL differs for different dose metrics. For length and width, the limits are determined by the aforementioned bioavailability limits. For length, given the default microplastic size range, LL and UL are equal to 1 and 5000 µm, respectively. If bioavailability relates to ingestion, the limits for width would range between 1 µm (LL) and the mouth opening of the organism (UL). For surface area and volume, UL and LL can be calculated using the appropriate ellipsoid equations (see Section 2.3), for which then the same minimum and maximum bioavailable values for length and width are used, while for height a value of 0.67 × width is used. For mass, the limits can be calculated by multiplying (bioavailable) ellipsoid volume with the average density (Table S3). For specific surface area, the surface area is divided by the mass. By combining Eqs. (2) to 4, the threshold effect concentration for the ERM of choice (EC_{env}) can be calculated.

Now that the threshold effect concentration (EC_{env}) and the exposure concentration (C_{env}) are aligned and scaled to the full 1 to 5000 µm microplastic size range, a consistent risk characterization can be done (numerical example, see Section S3). Note that the characterization is based on number concentrations, which may seem counterintuitive if the actual ERM would relate to e.g. volume, mass or area. However, we can easily convert exposure and effect number concentrations into for instance equivalent volume, mass or area concentrations (µm^3/L, µg/L, µm^2/L) by multiplying them with the mean value of their respective power law distributions (Eq. (4)), which yields:

$$\begin{aligned} C_{env,ERM,x} &= \mu_{x,\ poly} \times C_{env} \text{ and} \\ EC_{env,ERM,x} &= \mu_{x,\ poly} \times EC_{env} \end{aligned} \tag{5}$$

In this case the limits LL and UL in $\mu_{x,\ poly}$ (Eq. (4)) would relate to the values of the ERM at the 1 and 5000 µm size limits, respectively, rather than to bioavailability limits. In the risk characterization ($C_{env,ERM,x}/EC_{env,ERM,x}$), however, $\mu_{x,\ poly}$ cancels out. Eq. (5) also defines the conversion of number to mass concentration or vice versa. Finally, the above procedure applies to one ERM at a time. However, microplastic particles are likely to cause multiple effects simultaneously, once their respective threshold effect concentrations are exceeded. This means that the approach offered here can be used to rank the impact thresholds for the different dose metrics of interest with the most sensitive one determining the ultimate risk.

4. Conclusions

Continuous power law distributions for microplastic particle characteristics length, width, area, volume, mass and specific surface area have been parameterized, taking new quality criteria for accuracy loss due to subsampling into account. We show how each of these particle characteristics links to a dose metric relevant for microplastic effect mechanisms. We found that distributions of these characteristics differed for marine and freshwater surface waters and sediments, waste water effluents and benthic freshwater biota. We demonstrated that distributions for particle size were polymer-specific. With the presented distributions and scaling laws, exposure data from environmental concentrations, as well as effect concentrations obtained in experiments using monodisperse particles, can be aligned and rescaled to obtain consistent risk characterizations that fully represent the multidimensionality of microplastic.

5. Contributors

MK, SP and AAK designed the study. Data was collected and (re-) analyzed by SP, SMM, CL and GG. Data analyses was done by MK. MK wrote the article, with substantial contribution from AAK and additional feedback and final approval of all authors.

Declaration of Competing Interest

The authors declare that they have no known competing financial interests or personal relationships that could have appeared to influence the work reported in this paper.

Acknowledgments & funding sources

We would like to thank Changgui Pan, Thomas Mani and all their co-authors for sharing their raw data. Also, we want to thank Nur Hazimah Mohamed Nor and Pablo Rodríguez-Sánchez for their feedback on different aspects of the manuscript.

MK, SMM and AAK were supported by the Dutch Technology Foundation TTW (project number 13940), with additional support from KWR, IMARES, NVWA, RIKILT, the Dutch Ministry of Infrastructure and the Environment, The Dutch Ministry of Health, Welfare and Sport, Wageningen Food & Biobased Research, STOWA, RIWA and the Dutch water boards (BTO Joint Research Program). CL was supported by a PhD scholarship from The German Federal Environmental Foundation (DBU).

Supplementary materials

Supplementary material associated with this article can be found, in the online version, at doi:10.1016/j.watres.2021.117429.

References

Abel, S.M., Primpke, S., Int-Veen, I., Brandt, A., Gerdts, G., 2021. Systematic identification of microplastics in abyssal and hadal sediments of the Kuril Kamchatka trench. Environ. Pollut. 269, 116095.

Au, S.Y., Bruce, T.F., Bridges, W.C., Klaine, S.J., 2015. Responses of Hyalella azteca to acute and chronic microplastic exposures. Environ. Toxicol. Chem. 34, 2564–2572. https://doi.org/10.1002/etc.3093.

Bakir, A., O'Connor, I.A., Rowland, S.J., Hendriks, A.J., Thompson, R.C., 2016. Relative importance of microplastics as a pathway for the transfer of hydrophobic organic chemicals to marine life. Environ. Pollut. 219, 56–65.

Bern, L., 1990. Size-related discrimination of nutritive and inert particles by freshwater zooplankton. J. Plankton Res. 12, 1059–1067.

Brandt, J., Fischer, F., Kanaki, E., Enders, K., Labrenz, M., Fischer, D., 2021. Assessment of subsampling strategies in microspectroscopy of environmental microplastic samples. Front. Environ. Sci. 8, 579676.

Burns, E.E., Boxall, A.B.A., 2018. Microplastics in the aquatic environment: evidence for or against adverse impacts and major knowledge gaps. Environ. Toxicol. Chem. 37, 2776–2796.

Clauset, A., Shalizi, C.R., Newman, M.E.J., 2009. Power-law distributions in empirical data. SIAM Rev. 51, 661–703.

Cózar, A., Echevarría, F., González-Gordillo, J.I., Irigoien, X., Ubeda, B., Hernández-León, S., Palma, A.T., Navarro, S., García-de-Lomas, J., Ruiz, A., Fernández-de-Puelles, M.L., Duarte, C.M., 2014. Plastic debris in the open ocean. Proc. Natl. Acad. Sci. USA 111, 10239–10244. https://doi.org/10.1073/pnas.1314705111.

de Ruijter, V.N., Redondo-Hasselerharm, P.E., Gouin, T., Koelmans, A.A., 2020. Quality criteria for microplastic effect studies in the context of risk assessment: a critical review. Environ. Sci. Technol. 54, 11692–11705.

Endo, S., Koelmans, A.A., 2016. Sorption of Hydrophobic Organic Compounds to Plastics in the Marine Environment: Equilibrium, in: Hazardous Chemicals Associated with Plastics in the Marine Environment. Springer, pp. 185–204.

Everaert, G., De Rijcke, M., Lonneville, B., Janssen, C.R., Backhaus, T., Mees, J., van Sebille, E., Koelmans, A.A., Catarino, A.I., Vandegehuchte, M.B., 2020. Risks of floating microplastic in the global ocean. Environ. Pollut. 267, 115499.

Frère, L., Maignien, L., Chalopin, M., Huvet, A., Rinnert, E., Morrison, H., Kerninon, S., Cassone, A.-L., Lambert, C., Reveillaud, J., 2018. Microplastic bacterial

communities in the Bay of Brest: influence of polymer type and size. Environ. Pollut. 242, 614–625.
Fubini, B., 1997. Surface reactivity in the pathogenic response to particulates. Environ. Health Perspect. 105, 1013–1020.
Gillespie, C.S., 2014. Fitting Heavy Tailed Distributions: The Powerlaw Package arXiv Prepr. arXiv1407.3492.
Godoy, V., Blázquez, G., Calero, M., Quesada, L., Martin-Lara, M.A., 2019. The potential of microplastics as carriers of metals. Environ. Pollut. 255, 113363.
Gray, A.D., Weinstein, J.E., 2017. Size-and shape-dependent effects of microplastic particles on adult daggerblade grass shrimp (Palaemonetes pugio). Environ. Toxicol. Chem. 36, 3074–3080.
Guthrie Jr,, G.D., 1997. Mineral properties and their contributions to particle toxicity. Environ. Health Perspect. 105, 1003–1011.
Jâms, I.B., Windsor, F.M., Poudevigne-Durance, T., Ormerod, S.J., Durance, I., 2020. Estimating the size distribution of plastics ingested by animals. Nat. Commun. 11, 1–7.
Kaandorp, M.L.A., Dijkstra, H.A., van Sebille, E., 2021. Modelling size distributions of marine plastics under the influence of continuous cascading fragmentation. Environ. Res. Lett. https://doi.org/10.1088/1748-9326/abe9ea.
Koelmans, A.A., Besseling, E., Foekema, E., Kooi, M., Mintenig, S., Ossendorp, B.C., Redondo-Hasselerharm, P.E., Verschoor, A., Van Wezel, A.P., Scheffer, M., 2017. Risks of plastic debris: unravelling fact, opinion, perception, and belief. Environ. Sci. Technol. 51, 11513–11519.
Koelmans, A.A., Mohamed Nor, N.H., Hermsen, E., Kooi, M., Mintenig, S.M., De France, J., 2019. Microplastics in freshwaters and drinking water: critical review and assessment of data quality. Water Res. 155, 410–422.
Koelmans, A.A., Redondo-Hasselerharm, P.E., Mohamed Nor, N.H., Kooi, M., 2020. Solving the nonalignment of methods and approaches used in microplastic research to consistently characterize risk. Environ. Sci. Technol. 54, 12307–12315.
Kögel, T., Bjorøy, Ø., Toto, B., Bienfait, A.M., Sanden, M., 2020. Micro-and nanoplastic toxicity on aquatic life: determining factors. Sci. Total Environ. 709, 136050.
Kooi, M., Besseling, E., Kroeze, C., van Wenzel, A.P., Koelmans, A.A., 2018. Modeling the fate and transport of plastic debris in freshwaters: review and guidance. Freshwater Microplastics. Springer, pp. 125–152.
Kooi, M., Koelmans, A.A., 2019. Simplifying microplastic via continuous probability distributions for size, shape, and density. Environ. Sci. Technol. Lett. 6, 551–557.
Lorenz, C., Roscher, L., Meyer, M.S., Hildebrandt, L., Prume, J., Löder, M.G.J., Primpke, S., Gerdts, G., 2019. Spatial distribution of microplastics in sediments and surface waters of the southern North Sea. Environ. Pollut. 252, 1719–1729.
Mani, T., Primpke, S., Lorenz, C., Gerdts, G., Burkhardt-Holm, P., 2019. Microplastic pollution in benthic midstream sediments of the Rhine River. Environ. Sci. Technol. 53, 6053–6062.
Mattsson, K., Björkroth, F., Karlsson, T., Hassellöv, M., 2021. Nanofragmentation of expanded polystyrene under simulated environmental weathering (thermooxidative degradation and hydrodynamic turbulence). Front. Mar. Sci. https://doi.org/10.3389/fmars.2020.578178.
Michel, C., Herzog, S., de Capitani, C., Burkhardt-Holm, P., Pietsch, C., 2014. Natural mineral particles are cytotoxic to rainbow trout gill epithelial cells in vitro. PLoS One 9, e100856.
Min, K., Cuiffi, J.D., Mathers, R.T., 2020. Ranking environmental degradation trends of plastic marine debris based on physical properties and molecular structure. Nat. Commun. 11, 1–11.
Mintenig, S.M., Kooi, M., Erich, M.W., Primpke, S., Redondo Hasselerharm, P.E., Dekker, S.C., Koelmans, A.A., van Wezel, A.P., 2020. A systems approach to understand microplastic occurrence and variability in Dutch riverine surface waters. Water Res. 176, 115723.
Mohamed Nor, N.H., Kooi, M., Diepens, N.J., Koelmans, A.A., 2021. Lifetime accumulation of microplastic in children and adults. Environ. Sci. Technol. 55 (8), 5084–5096. https://doi.org/10.1021/acs.est.0c07384.
Newman, M.E.J., 2005. Power laws, Pareto distributions and Zipf`s law. Contemp. Phys. 46, 323–351.
Pan, C.-G., Mintenig, S.M., Redondo-Hasselerharm, P.E., Neijenhuis, P., Yu, K., Wang, Y., Koelmans, A.A., 2021. Automated uFTIR imaging demonstrates taxon-specific and selective uptake of microplastic by freshwater invertebrates. Environ. Sci. Technol. 55 https://doi.org/10.1021/acs.est.1c03119.
Primpke, S., Cross, R.K., Mintenig, S.M., Simon, M., Vianello, A., Gerdts, G., Vollertsen, J., 2020a. Toward the systematic identification of microplastics in the environment: evaluation of a new independent software tool (siMPle) for spectroscopic analysis. Appl. Spectrosc. 74, 1127–1138.
Primpke, S., Dias, P.A., Gerdts, G., 2019. Automated identification and quantification of microfibres and microplastics. Anal. Methods 11, 2138–2147.
Primpke, S., Fischer, M., Lorenz, C., Gerdts, G., Scholz-Böttcher, B.M., 2020b. Comparison of pyrolysis gas chromatography/mass spectrometry and hyperspectral FTIR imaging spectroscopy for the analysis of microplastics. Anal. Bioanal. Chem. 412, 8283–8298.
Primpke, S., Wirth, M., Lorenz, C., Gerdts, G., 2018. Reference database design for the automated analysis of microplastic samples based on Fourier transform infrared (FTIR) spectroscopy. Anal. Bioanal. Chem. 410, 5131–5141.
Rauchschwalbe, M.-.T., Fueser, H., Traunspurger, W., Höss, S., 2021. Bacterial consumption by nematodes is disturbed by the presence of polystyrene beads: the roles of food dilution and pharyngeal pumping. Environ. Pollut. 273, 116471.
Riediker, M., Zink, D., Kreyling, W., Oberdörster, G., Elder, A., Graham, U., Lynch, I., Duschl, A., Ichihara, G., Ichihara, S., 2019. Particle toxicology and health-where are we? Part. Fibre Toxicol. 16, 1–33.
Rochman, C.M., Brookson, C., Bikker, J., Djuric, N., Earn, A., Bucci, K., Athey, S., Huntington, A., McIlwraith, H., Munno, K., 2019. Rethinking microplastics as a diverse contaminant suite. Environ. Toxicol. Chem. 38, 703–711.
Schmid, O., Stoeger, T., 2016. Surface area is the biologically most effective dose metric for acute nanoparticle toxicity in the lung. J. Aerosol Sci. 99, 133–143.
Schwarze, P.E., Øvrevik, J., Hetland, R.B., Becher, R., Cassee, F.R., Låg, M., Løvik, M., Dybing, E., Refsnes, M., 2007. Importance of size and composition of particles for effects on cells in vitro. Inhal. Toxicol. 19, 17–22.
Simon, M., van Alst, N., Vollertsen, J., 2018. Quantification of microplastic mass and removal rates at wastewater treatment plants applying Focal Plane Array (FPA)-based Fourier Transform Infrared (FT-IR) imaging. Water Res. https://doi.org/10.1016/J.WATRES.2018.05.019.
Stoeger, T., Reinhard, C., Takenaka, S., Schroeppel, A., Karg, E., Ritter, B., Heyder, J., Schulz, H., 2006. Instillation of six different ultrafine carbon particles indicates a surface area threshold dose for acute lung inflammation in mice. Environ. Health Perspect. 114, 328–333.
Tran, C.L., Buchanan, D., Cullen, R.T., Searl, A., Jones, A.D., Donaldson, K., 2000. Inhalation of poorly soluble particles. II. Influence of particle surface area on inflammation and clearance. Inhal. Toxicol. 12, 1113–1126.
Velzeboer, I., Kwadijk, C., Koelmans, A.A., 2014. Strong sorption of PCBs to nanoplastics, microplastics, carbon nanotubes, and fullerenes. Environ. Sci. Technol. 48, 4869–4876.
White, E.P., Enquist, B.J., Green, J.L., 2008. On estimating the exponent of power-law frequency distributions. Ecology 89, 905–912.
Wright, S.L., Kelly, F.J., 2017. Plastic and human health: a micro issue? Environ. Sci. Technol. 51, 6634–6647.
Ziajahromi, S., Kumar, A., Neale, P.A., Leusch, F.D.L., 2017. Impact of microplastic beads and fibers on waterflea (Ceriodaphnia dubia) survival, growth, and reproduction: implications of single and mixture exposures. Environ. Sci. Technol. 51, 13397–13406.